Research Square

Preprints are preliminary reports that have not undergone peer review.
They should not be considered conclusive, used to inform clinical practice,
or referenced by the media as validated information.

Amorphous Silica and Drought Stress Mitigation: Unraveling Phenological Dynamics, Carbon-Water Balance, and Crop Resilience

Wael Al Hamwi

Wael.Alhamwi@zalf.de

Leibniz Centre for Agricultural Landscape Research

Mathias Hoffmann

Leibniz Centre for Agricultural Landscape Research

Jörg Schaller

Leibniz Centre for Agricultural Landscape Research

Rainer Remus

Leibniz Centre for Agricultural Landscape Research

Adrian Dahlmann

Leibniz Centre for Agricultural Landscape Research

Maren Dubbert

Leibniz Centre for Agricultural Landscape Research

Article

Keywords: Amorphous silica, drought, greenhouse experiment, spring barley, phenological stages, carbon and water cycle dynamics

Posted Date: October 14th, 2026

DOI: https://doi.org/10.21203/rs.3.rs-11116050/v1

License: This work is licensed under a Creative Commons Attribution 4.0 International License. Read Full License

Additional Declarations: No competing interests reported.

Abstract

Amorphous silica (ASi) is increasingly recognized for its potential to improve plant resilience to abiotic stress, especially drought. However, because drought affects crop physiology as well as its carbon and water cycling differently depending on when drought occurs during plant development, the effects of ASi across key phenological stages remain poorly understood. In a greenhouse experiment, we investigated whether ASi as a soil amendment mitigates drought stress in spring barley (Hordeum vulgare L., variety: Planet) during three key phenological stages: stem elongation, flowering, and grain filling. A factorial design was used, combining two levels of ASi (0 as control and 1 g per 100 g of dry soil) with four water regimes: a well-watered reference and drought imposed during stem elongation, flowering, or grain filling. Carbon and water flux dynamics were monitored throughout the experiment by measuring CO_2 exchange and evapotranspiration using an automated soil-plant-atmosphere enclosure system, while soil water dynamics were tracked continuously with TOMST sensors. Plant responses to drought were assessed by daily measurements of stomatal conductance, leaf water potential, abscisic acid, and soil matric potential during drought. At the end of the growing period, biomass and grain yield were determined. ASi increased soil water retention over time and reduced drought-induced stress across growth stages. Drought effects were strongest during flowering and grain filling, whereas plants exposed to drought at stem elongation recovered fully and showed no yield reduction, irrespective of their ASi treatment. In contrast, drought during reproductive stages caused early senescence, poor recovery, and strong yield loss in control plants. These effects were substantially reduced by ASi, which maintained higher leaf water potential, stomatal conductance, evapotranspiration, and CO_2 uptake, while reducing abscisic acid accumulation. ASi also improved post-drought recovery and largely preserved yield under reproductive-stage drought. These results show that ASi can mitigate drought effects, especially during drought-sensitive reproductive stages, by helping sustain plant function during water shortages and delaying the onset of physiological stress.

Introduction

Drought causes significant production losses, particularly for cereals such as wheat and barley, thereby threatening global food security[1,2]. The physiological impact of drought is determined not only by the magnitude of water deficiency but also by its coincidence with critical phenological stages[3,4]. Even short-term drought stress can disrupt pollination, decrease assimilation and nutrient transfer to developing seeds, and accelerate senescence [3,5,6,7].

Amorphous silica (ASi), a non-crystalline form of silica that commonly occurs in soils in hydrated form (SiO_2.nH)[8], has emerged as a promising tool for enhancing soil properties and supporting plant resilience under both biotic and abiotic stress [8,9,10,11,12,13,14]. Natural soils contain around 1–6% ASi; however, agricultural soils are often depleted of ASi, containing less than 1% or near zero [8,15]. This depletion is driven by the high ASi uptake rates of crops like wheat and barley, combined with the continuous removal of the ASi stored in biomass through harvest without its sufficient replacement [16,17,18].

ASi can affect both soils and plants. In soils, ASi can increase soil water-holding capacity and improve hydraulic conductivity, thereby helping maintain root access to water, especially in coarse-textured soils [19,20,21]. In plants, ASi can promote root development [22,23] and improve root hydraulic conductance [24,25], thereby

reducing negative leaf water status during drought stress [26]. Moreover, ASi modulates hormonal stress signaling, including abscisic acid (ABA) signaling, by regulating genes involved in ABA biosynthesis and degradation. This can reduce ABA accumulation under stress and help maintain stomatal regulation during drought [27,28].

Despite these reported benefits, gaps still exist in our mechanistic and agronomic understanding of ASi. Research has mainly focused on the vegetative phenological stage, leaving the effects of ASi during key reproductive phenological stages (e.g., flowering and grain filling) largely underexplored [29,30]. More critically, we lack a comprehensive understanding of the dynamics that control how ASi supports both immediate stress mitigation and subsequent recovery. Because rapid changes in carbon uptake, transpiration, and water status happen over short periods, standard sampling methods often miss these transient physiological shifts. This absence of high temporal resolution data makes it difficult to determine how ASi provides resilience, limiting our ability to forecast crop performance in increasingly unpredictable climates.

Here, we address these gaps with a controlled greenhouse experiment that applies drought at three phenological stages in barley grown in sandy soil, with and without ASi as soil amendment. By using an automatic soil-plant-atmosphere enclosure system (Al Hamwi et al., 2024)[31], we aim to quantify drought responses and post-drought recovery across key growth stages, assessed through high-frequency carbon and water fluxes, soil and plant water status, and physiological indicators. We hypothesize that: 1) ASi mitigates drought impact at all key plant growth stages (stem elongation, flowering, and grain filling). 2) ASi speeds up post-drought recovery. 3) ASi benefits will translate into preserved or higher grain yield at harvest.

Material and methods

Experimental design, soil preparation, and growth conditions

To investigate the ability of ASi amendment to mitigate drought stress during key phenological stages, a greenhouse experiment with spring barley (Hordeum vulgare L.; variety: Planet) was conducted in the greenhouse at ZALF, Müncheberg, Germany (52.5164° N, 14.1190° E). For the greenhouse experiment, a factorial design was used, combining two ASi levels (0 and 1 g per 100 g of dry soil) with four drought groups: well-watered reference, drought at stem elongation, drought at flowering, and drought at grain filling. This yielded eight treatments, each replicated four times, for a total of 32 pots (inner diameter 20 cm, height 19 cm). Pots were arranged in a completely randomized design across three columns and re-randomized weekly to minimize positional effects. The soil used in this study was collected from the topsoil of the experimental field at ZALF. The field site has previously been classified as an Albic, Lamellic Arenosol (Aric). To reduce the soil's water-holding capacity, thereby accelerating soil drying and pushing the soil–plant system toward extreme water stress, the collected topsoil was mixed after being sieved through a 2 mm mesh with pure quartz sand (40% by volume). The resulting soil mixture had a final texture of 95% sand, 2% silt, and 3% clay, and contained 0.069% organic matter. Before adding ASi, the soil contained 1.6 mg ASi per gram of dry soil, as determined using a cold NaOH extraction after Stein et al. (2024)[32]. Each pot was filled with 8 kg of air-dried soil mixture. For pots treated with ASi, an additional 80 g ASi (Aerosil 300, Evonik Industries AG, Essen, Germany), equivalent to 1% of the soil dry mass, was added to each pot and mixed thoroughly by hand into the 8 kg soil batch until the amendment was no longer visibly distinguishable, resulting in a total mass of 8.08 kg per pot.

To negate differences in seed weight, barley seeds were selected within a narrow weight range (60–80 mg). Seeds were pre-germinated on moist filter paper in Petri dishes. Once the cotyledons formed, the seedlings were transferred to pots, with each pot containing 20 seedlings. Seedlings were planted at equal radial distances using a standard template to ensure consistent spacing and minimize edge effects and competition. The greenhouse air temperature was maintained at 19°C during the 16-hour light period and 14°C during the 8-hour dark period. The relative humidity averaged 43% during the day and 50% at night. An artificial light source was used, and the light intensity at the canopy level and the gas flux measurement system were adjusted to 350 µmol m^{-2} s^{-1} at the start of the experiment. To ensure sufficient nutrient availability, a commercial mineral fertilizer (WOPIL) containing nitrogen (N, 14%; composed of 8% nitrate-N and 6% ammonium-N), phosphorus (as P_2O_5, 6%), potassium (as K_2O, 24%), magnesium (as MgO, 3%), and micronutrients (B, Fe, Cu, Mn, Mo, Zn) was dissolved in irrigation water and applied at a rate of 1.5 g per pot per application. Fertilization started one month after planting and was repeated every 15 days, for a total of 4 applications.

Soil water content (SWC) was initially adjusted to 70% of field capacity to provide suitable moisture conditions for barley growth [33]. Thereafter, all treatments received the same amount of water daily. The daily water amount added was determined from the mean daily water loss of the 16 control pots, estimated by pot weighing without accounting for plant biomass. Thus, it was aimed to maintain similar moisture dynamics among treatments. To simulate drought across different phenological stages, no water was provided to the targeted treatment group for 5 consecutive days. At the end of each drought period, the control pots in the affected group were weighed, and the average water loss relative to the initial SWC was determined. This amount of water was then uniformly applied to the group's control and ASi-treated pots, ensuring a consistent rehydration strategy across treatments.

Soil water content, soil water potential, leaf water potential, and stomatal conductance measurements

During the greenhouse experiment, soil water content and temperature were measured continuously at 15-minute intervals using a TOMST sensor (TMS-4, TOMST, Czech Republic) placed in the center of each pot. Soil matric potential (SMP) was measured with a TEROS-21 sensor (METER Group, Inc.), also placed centrally in the pot (up to a soil depth of 9 cm). Leaf water potential (LWP) was measured using a Scholander pressure chamber (SoilMoisture Equipment Corp., Santa Barbara, CA, USA). For each LWP measurement, the third fully expanded leaf from the top of a plant in each pot was cut, sealed in the measuring chamber, and pressurized until xylem sap visibly emerged from the cut surface. The applied pressure was recorded as the LWP [34]. In case the applied pressure exceeded 6.5 MPa, the measurement was stopped, and the LWP value was reported as 6.5 MPa. Stomatal conductance (g_s) was measured using a SC-1 Leaf Porometer (METER Group, Inc.), where g_s was measured on the lower side (abaxial surface) of the third leaf [35]. The third leaf measurement was used to represent the plant's overall g_s. Measurements of SMP, LWP, and g_s were conducted only during the 5-day drought period at midday (between 12:00 and 13:00).

Hormone stress abscisic acid (ABA)

For ABA analysis, the third fully expanded leaf from the apex of a plant in each pot was cut, immediately frozen in liquid nitrogen, and stored at -80°C until analysis. Freeze-dried and ground samples (about 10 mg of dry tissue) were extracted with ice-cold 50% acetonitrile containing internal standards and purified by solid-phase extraction using Oasis Prime HLB cartridges, following a modified protocol based on Šimura et al. (2018)[36]. Extracts were then dried, reconstituted in 30% acetonitrile with 0.1% formic acid, and ABA was quantified by UHPLC-ESI-MS/MS as described by Eggert and Von Wiren (2017)[37]. The ABA analysis was performed in the laboratory of the Leibniz Institute of Plant Genetics and Crop Plant Research, Gatersleben, Germany.

CO and evapotranspiration (ET) flux measurements

CO_2 and ET fluxes were measured using a low-cost, automated chamber system as described in detail by Al Hamwi et al. (2024)[31]. In short, this system consists of 10 enclosed, transparent chambers (PVC; 180 cm x 40 cm x 60 cm) that can each house 1 pot with a plant (as a soil-plant atmosphere system), for a total of 10 pots at the same time. The chambers are connected to an infrared gas analyzer (LI-850, LI-COR Biosciences, USA) via a multiplexer.

Outside the drought periods, each pot was measured once per week over a full 24-hour cycle. Pots were randomly assigned to chambers. To minimize chamber-specific bias, pots belonging to the same treatment combination (i.e., the same drought group and ASi level) were not measured within the same cycle, and no chamber was repeatedly assigned to the same treatment combination across cycles. During drought periods, the regular weekly schedule was suspended. Pots subjected to drought were measured continuously throughout the drought, in order to capture rapid changes in CO_2 exchange and ET as water stress progressed.

To determine the CO_2 and ET fluxes, the concentration changes of CO_2 and H_2O in the chamber headspace were measured every 5 seconds for a period of 5 minutes after the chamber was automatically sealed airtight. Daytime measurements are used to estimate net ecosystem exchange (NEE) while nighttime measurements are used to estimate ecosystem respiration (R_{eco}). Additionally, environmental variables, including air temperature inside and outside the chamber (SHT31 sensor) and photosynthetically active radiation (PAR; SKP215, Skye Instruments Ltd., UK), were recorded at 5-second intervals.

CO and ET flux calculations and gap filling

CO_2 and ET fluxes were calculated with a modular R script described by Hoffmann et al. (2015)[38] for CO_2 and by Dahlmann et al. (2023)[39] for ET. Before flux calculation, the first and last 10% of each flux measurement were excluded, thus avoiding disturbances caused by chamber closure, short pressure changes, and unstable air mixing inside the chamber. In addition, CO_2 concentrations were corrected for water vapor interference following Webb et al. (1980)[40] and Hupp (2011)[41]. Fluxes were then calculated from the linear change in chamber headspace concentration over time using the ideal gas law. To obtain the most reliable concentration change during chamber closure, the R script did not use the full closure period directly but applied a variable moving window to each flux measurement. In our case, window lengths ranging from 0.5 to 5 min were used, yielding several possible CO_2 and ET fluxes for each chamber closure. These fluxes were then screened using a set of quality criteria, including the assumptions required for linear regression, namely normality,

homoscedasticity, and linearity, a significant regression slope at $p \leq 0.1$, stable chamber conditions with a within-window air temperature range not exceeding ± 1.5 K and, during daytime measurements, a PAR deviation not exceeding ± 20% of the mean, and the absence of outliers beyond ± 6 times the interquartile range. Only fluxes fulfilling all criteria were retained. When more than one valid flux was available for a given chamber closure, the flux with the steepest slope and the closest timing to chamber closure was selected for further analysis.

For gap filling, empirical models were used. R_{eco} was modeled with a temperature-dependent Arrhenius-type function according to Lloyd et al. (1994)[42]. Separate models were fitted using air temperature measured inside and outside the chamber, as well as soil temperature. The final R_{eco} model was selected as the one with the lowest Akaike information criterion. GPP was modeled with a PAR-dependent rectangular hyperbolic light-response function following [38,43,44]. Because GPP was not measured directly, it was calculated as the difference between measured NEE and modeled R_{eco}. When the rectangular hyperbolic model did not produce significant parameter estimates, a non-rectangular hyperbolic light-response function was used instead, following Gilmanov et al. (2007, 2013)[45,46]. If no valid fit could be obtained, average flux values were used for R_{eco} and GPP. Based on the selected models and continuous temperature and PAR data, R_{eco}, GPP, and NEE were then reconstructed at half-hourly resolution over the full measurement period. These parameter sets were generated per treatment and measurement day.

For ET, a data-driven modeling approach using a random forest (RF) model following Dahlmann et al. (2023) [39] was applied. Air temperature, soil temperature, PAR, relative humidity, and SWC were utilized as predictors within the RF model. Validation was conducted via 10-fold cross-validation to assess predictive stability. The resulting performance was assessed using MAE and R^2, consistent with the performance criteria defined in Dahlmann et al. (2023). One TOMST sensor failed, resulting in gaps in soil water content lasting longer than 3 consecutive days but shorter than 7 days. Because of this issue, one ASi-treated pot in the GR group was excluded from the ET balance and the ecosystem water use efficiency (WUE_{eco}) analysis. WUE_{eco} was calculated as the ratio of NEE to ET, following Anapalli et al. (2023)[47] and Zhang et al. (2025)[48].

Biomass harvesting and analysis

At the end of the growing season, the whole plants were harvested manually and separated into grains, leaf blades, and stems. Roots were harvested manually after the aboveground biomass had been removed. The entire air-dried soil from each pot was carefully taken out and placed on a 2 mm sieve. The soil was then gently shaken for 5 minutes to separate most of the roots from the soil, leaving the roots retained on the sieve. After sieving, the passed soil was visually inspected by hand for an additional 5 minutes to recover any remaining roots that had passed through or remained mixed with the soil. These roots were then added to the previously collected root sample. Each part of the harvested plant was oven-dried at 50°C for 48 h, then weighed to determine dry biomass. From the grain yield and shoot biomass, the harvest index (HI) was calculated according to the following Eq. (1)[49]:

$$\mathrm{HI} = \frac{\text{Grain yield}}{\text{Grain yield} + \text{Shoot biomass}} \times 100$$

1

Dried material from each plant part was analyzed for total carbon (C_t) and nitrogen (N_t) following standard protocols (DIN ISO 10694 for C_t and DIN ISO 13878 for N_t) using a CNS analyzer (CNS928-MLC, Leco Instruments GmbH) at the central laboratory of ZALF. For ASi content, 0.03g of dried samples were digested in 30mL of Na_2CO_3 solution at 85°C for 5 hours. The extract was then filtered through a 0.2 mm membrane filter, following the procedure described by Puppe et al. (2023)[50]. ASi concentrations in the filtered solutions were determined using inductively coupled plasma optical emission spectrometry (ICP-OES; Varian Vista-Pro Radial, Palo Alto, CA, USA).

Statistical analysis

All statistical analyses were performed in R version 4.5.0 (R Core Team, 2025). For g_s and LWP, two-way ANOVA models were used to test the effects of ASi treatments and sampling day during drought, as well as their interaction. HI, yield, and dry biomass were analyzed separately using a two-way ANOVA with ASi treatment and drought group as factors. Homogeneity of variances was verified using Levene's test, and normality of the residuals was assessed with the Shapiro-Wilk test. Post hoc differences were determined using Tukey's HSD test, with significance set at $p < 0.05$ and different letters indicating statistically distinct groups. For SWC and SMP, ASi and Control treatments were compared separately within each phenological stage and on each drought day using Welch's two-sample t-test, which does not assume equal variance between treatments. Statistical significance was assessed at $p < 0.05$.

For the ABA-SMP and LWP-SMP relationship, linear mixed effects were fitted separately for each drought stage, with treatment, SMP, and their interaction as fixed effects and pot as a random effect. Differences between ASi and Control slopes were tested using estimated marginal trends. Because the g_s-SMP relationship was nonlinear, generalized additive mixed models were fitted separately for each stage, including treatment-specific smooth terms and pot as a random effect. Statistical significance was set at $p < 0.05$.

For NEE and ET, linear mixed-effects models were fitted with treatment, growth stage, and drought phase as fixed effects and pot as a random factor. Pairwise contrasts between treatments were obtained using estimated marginal means (emmeans package). Model assumptions were verified by residual diagnostics, and permutation tests were used when necessary to account for non-normality.

Results

ASi enhanced soil water retention at reproductive stages

SWC and SMP responded differently to ASi depending on the stage at which drought was imposed. During drought at ST (Fig. 1B), SWC did not differ significantly between ASi-treated and control pots ($p > 0.05$). However, the corresponding SMP (Fig. 1E) declined faster in ASi-treated pots, reaching significantly more negative values on the last two days of drought ($p < 0.05$). Thus, despite similar SWC, water was held under greater tension in ASi-treated pots.

During drought at FL and GR, the pattern differed (Fig. 1C and D). ASi-treated pots maintained significantly higher SWC than control pots throughout the drought and remained at less negative SMP, which was significant

on days 3 and 4 at FL and days 2 and 3 at GR ($p < 0.05$) (Fig. 1F and G). These results were consistent with the measured water retention curves, in which ASi-treated pots retained more water than control pots at a given SMP (Appendix A; Fig. 1A).

After rewetting, the soil in ASi-treated pots returned to pre-drought levels, whereas control pots showed higher SWC after drought, reflecting plant senescence and the absence of transpiration. Total irrigation water applied averaged 646.25 ± 8.30 mm, with minor differences between drought groups. These minor differences resulted from stage-specific interruptions in watering during the 5-day drought and the subsequent recovery of lost water, rather than from differences in the overall irrigation schedule.

ASi sustained higher ET and LWP under drought at reproductive stages

Under reference conditions (Fig. 2-A), ET followed a similar pattern in ASi-treated and control pots, with no significant differences across the experimental period ($p > 0.05$). During drought at the ST (Fig. 2-B), ET declined in response to the imposed drought and was slightly higher, but not significantly different ($p > 0.05$) in ASi-treated pots compared to control pots. Also, the differences between treatments were non-significant both before and after the drought. The corresponding LWP (Fig. 2-E) declined in both treatments, with no consistent ASi effect until the last day, when ASi-treated plants had significantly less negative LWP (i.e., higher water potential) than controls. In contrast, during drought at FL and GR stages (Fig. 2C and D), ET differed significantly between treatments. Drought caused a sharp decline in ET in both stages, but ASi-treated pots maintained higher ET throughout the drought period ($p < 0.001$). LWP patterns (Fig. 2F and G) mirrored ET, with ASi-treated plants sustaining less negative (i.e., higher) water potentials than controls as drought progressed ($p < 0.001$). Additionally, seasonal sums (Table.1) show no ASi effect, with neither cumulative ET nor WUE_{eco} differing significantly between treatments in any drought group ($p > 0.05$, TukeyHSD, $n = 4$).

ASi buffered drought induced stress signals

Across all key phenological stages, ABA concentration increased as SMP declined (Fig. 3A, B, and C). During the drought at ST and FL, the slope of the ABA-SMP relationship differed significantly between ASi-treated and control pots ($p < 0.001$). In both stages, the slope was lower under ASi, indicating a weaker association between ABA concentration and soil matric potential under ASi.

LWP declined as SMP became more negative (Fig. 3D, E, and F). The LWP-SMP slope differed significantly between ASi-treated and control plant pots (ST: $p = 0.015$; FL: $p = 0.025$; and GR: $p < 0.001$). At all three stages, the slope was lower under ASi, indicating a weaker decline in LWP as SMP became more negative.

g_s changed nonlinearly with SMP (Fig. 3G, H, and I). Across ST, FL, and GR, g_s generally declined as SMP became more negative. However, only at ST did the g_s-SMP relationship differ significantly between ASi-treated and control pots ($p < 0.05$), indicating higher g_s under ASi.

ASi sustained higher CO_2 uptake during and after drought in reproductive stages

NEE showed a distinct seasonal trend across treatments and drought groups. Under reference conditions (Fig. 4-A), NEE patterns were similar in ASi-treated and control pots, with no significant differences throughout the experiment ($p > 0.05$). At ST (Fig. 4-B), NEE declined in response to drought, but no treatment effect was detected. No significant treatment differences were found also before or after drought. Consistent with this, g_s during drought (Fig. 4E) declined moderately in both treatments, again without significant differences. In the FL (Fig. 4-C), ASi-treated pots initially had significantly higher NEE than the control ($p < 0.05$), and no difference was observed during drought ($p > 0.05$). In the GR stage (Fig. 4-D), NEE was similar between treatments before drought ($p > 0.05$), but during drought, ASi-treated pots showed significantly lower NEE than the control ($p < 0.001$). Corresponding gs in ASi-treated pots for both groups (FT and GR) (Fig. 4F and G) was higher than in the control as drought progressed but was significantly higher only on the third day of drought. After drought, in both FL and GR, NEE in control pots approached zero and entered senescence, whereas ASi-treated pots recovered from drought ($p < 0.001$), resumed net carbon uptake, and continued physiological development before senescence, indicating a greater capacity for post-stress recovery. Additionally, seasonal totals (Table 1) showed no ASi effect, and cumulative NEE did not differ significantly between treatments in any drought group ($p > 0.05$, TukeyHSD, $n = 4$). However, within the control treatment, the FL and GR groups had significantly higher cumulative NEE (i.e., lower net carbon uptake) than the REF.

ASi reduced yield loss in reproductive stages and increased shoot biomass

HI was affected by drought timing and ASi treatment (Fig. 5a), with ASi-treated pots having significantly higher HI than the Control treatment at FL and GR ($p < 0.001$), but lower than the Control treatment at REF and ST, though not significantly. Grain yield also differed significantly by drought group and treatment ($p < 0.001$) (Fig. 5b). The highest yields were observed in REF and ST, which did not differ significantly. In the control treatment, drought at FL or GR caused significant yield losses of 65.4% ± 2.6% and 68.8% ± 2.2%, respectively, relative to the Control treatment in the REF group. ASi significantly mitigated these losses at both FL and GR, producing yields comparable to the reference group (ASi-FL and ASi-GR yielded only 19.7% ± 5.3% and 18.3% ± 6.2% below ASi-REF, respectively). Accordingly, ASi increased yield relative to the corresponding control by 142.6% ± 22.3% at FL and 173.5% ± 25.7% at GR, while the increases were small in ST (9.2% ± 4.6%) and REF (4.5% ± 4.6%). Shoot dry biomass showed a different response pattern (Fig. 5c). ASi-treated pots had significantly higher shoot dry biomass than control pots by 22.3% ± 3.8% in REF, 23.4% ± 3.1% in ST, and 37.5% ± 5.9% in FL, whereas it was not significantly higher in GR (2.7% ± 5.6%). Within the ASi treatment, ST and FL pots did not differ significantly in shoot dry biomass from REF, whereas GR differed significantly from REF. Within the control treatment, FL pots differed significantly from ST and GR pots but not from REF. Also, REF, ST, and GR pots did not differ significantly from one another.

Table 1

Mean values and standard errors of cumulative seasonal net ecosystem exchange (NEE, g C m^{-2} d^{-1}) and evapotranspiration (ET, mm d^{-1}), ecosystem water use efficiency (WUE_{eco}, g C m^{-2} mm^{-1} H_2O), and carbon and nitrogen content (%) in the shoot, as well as ASi content (%) in the upper three leaves ($ASi_{3leaves}$), lower leaves (ASi_{leaves}), and stem (ASi_{Stem}) for both treatments (ASi and control) across the four different drought groups [REF: Reference; ST: Stem elongation; FL: Flowering; GR: Grain filling].

Group	Treatment	NEE	ET	WUE_{eco}	C_{shoot}	N_{shoot}	$ASi_{3leaves}$	ASi_{leaves}	ASi_{Stem}
REF	**ASi**	-639.04 ± 82.41	418.67 ± 8.94	1.54 ± 0.22	14.09 ± 0.54	0.15 ± 0.01	22.13 ± 1.44	12.16 ± 0.46	5.81 ± 1.84
	Control	-647.13 ± 29.04	457.06 ± 20.11	1.42 ± 0.03	13.16 ± 0.35	0.15 ± 0.00	2.10 ± 0.09	1.99 ± 0.06	0.21 ± 0.02
ST	**ASi**	-678.00 ± 51.34	432.88 ± 15.61	1.57 ± 0.11	14.55 ± 0.24	0.16 ± 0.00	23.28 ± 1.02	12.27 ± 0.53	4.02 ± 0.03
	Control	-525.05 ± 31.69	439.06 ± 19.49	1.20 ± 0.08	13.12 ± 0.32	0.17 ± 0.01	2.27 ± 0.06	1.81 ± 0.13	0.27 ± 0.05
FL	**ASi**	-498.46 ± 39.42	422.97 ± 12.63	1.19 ± 0.13	13.68 ± 0.61	0.16 ± 0.01	19.38 ± 0.86	11.09 ± 0.39	3.45 ± 0.38
	Control	-410.34 ± 20.64	386.72 ± 20.96	1.07 ± 0.09	11.05 ± 0.08	0.26 ± 0.01	2.28 ± 0.18	2.13 ± 0.14	0.29 ± 0.03
GR	**ASi**	-477.02 ± 39.13	440.79 ± 28.27	1.04 ± 0.08	12.48 ± 0.66	0.16 ± 0.01	17.82 ± 1.51	9.96 ± 0.75	2.51 ± 0.44
	Control	-338.35 ± 56.76	343.42 ± 33.36	0.96 ± 0.08	13.55 ± 0.26	0.38 ± 0.01	1.82 ± 0.17	1.67 ± 0.15	0.24 ± 0.02

Discussion

Recently, ASi has emerged as a promising soil amendment for mitigating the effects of drought [51]. However, studies evaluating the impact of ASi under natural conditions and throughout the full crop cycle are rare. Instead, most studies focus on controlled experiments, often over short drought periods and at early vegetative stages rather than across the full crop cycle under more realistic conditions. This restricts a comprehensive understanding of the effects and feedback ASi amendments can have. Here, we conducted a greenhouse experiment, growing spring barley in sandy soil (benefiting most from ASi amendment[52]). The experiment included 8 treatments: two levels of ASi (0 and 1 g ASi per 100 g dried soil) and four drought groups (well-watered REF, drought imposed during ST, FL, and GR). This enabled us to study the impact of ASi on soil water storage, including potential cumulative effects, as well as the explicit impact of ASi on barley during distinct phenological stages. In addition, we studied the recovery phase and harvested all treatments only after

ripening and senescence, allowing us to link physiological responses during and after drought to agronomic parameters such as yield.

Across all drought groups, ASi-treated pots showed lower drought stress than the control. Under drought, ASi plants maintained a less negative LWP, indicating better plant water status and lower water limitation [53,54]. At the same time, ASi plants accumulated less ABA in their leaves, a drought hormone stress that normally rises during soil drying and drives stomatal closure[55]. Together, these responses support our first hypothesis that ASi reduces the impacts of drought across key plant phenological stages. At the end of each drought period, we rewatered the pots and observed their recovery. We define recovery as the resumption of carbon assimilation and transpiration after rewetting[56] as reflected in NEE and ET, along with soil water dynamics, which can indicate plant water uptake. Our results from the recovery phase partially support our second hypothesis. ASi speeds up post-drought recovery, as observed at FL and GR, but not at ST. Finally, the yield results can support our third hypothesis, mainly through grain yield preservation rather than a clear additional yield gain. This suggests that the main agronomic benefit of ASi in our experiment was not to increase grain yield under favorable conditions, but to buffer drought-induced grain yield losses when water limitation occurred during critical growth stages, making agriculture more sustainable under drought[57].

A key result beyond our initial hypotheses was that plant stress responses to drought were strongly phenologically stage-dependent. Stress responses were clearly more moderate at ST than at FL and GR, which agrees with the higher sensitivity of productive stages to water limitation. This pattern is important because it shows that the effect of ASi can not be understood without considering when drought occurs during crop development.

At ST, drought intensity was insufficient to cause lasting physiological damage. After rewetting, both ASi-treated and control plants recovered rapidly, as indicated by ET and NEE (Figs. 2 and 4). Furthermore, no significant differences between the treatments were observed in ET or NEE after the drought period, and the final yield was not reduced in either treatment (Fig. 5). These results suggest that ASi has no or only a limited effect on accelerating plant recovery at this stage. Our findings are also supported by Abid, M. et al. (2018)[6], which shows that mild drought at vegetative growth stages often allows rapid recovery when hydraulic damage is limited. At this stage, ASi therefore had only a limited effect on the speed of recovery, as the control plants also recovered fully.

In contrast, drought at FL and GR was severe enough to strongly suppress plant activity in the control treatment. The control plants progressed toward senescence, indicated by near-zero NEE and decreased ET, likely due to strongly reduced plant transpiration. Additionally, higher post-drought SWC in control plants likely reflects reduced transpiration and plant water uptake. This pattern aligns with premature senescence in the control treatment. However, ASi-treated plants resumed growth and continued to develop after drought, as evidenced by the recovery of ET and NEE (Figs. 2 and 4). This suggests that ASi delayed the onset of critical stress, reduced the time spent below damaging thresholds, and helped plants maintain functional activity until rewetting. These findings also align with the general view that reproductive stages are particularly vulnerable to drought because water limitations during this period can reduce flowering rate, fertilization, and grain development [3,58].

The harvest results confirm this stage-dependent pattern. HI (as an indicator of the ratio of grain yield to total aboveground biomass) declined strongly in the control treatment at FL and GR because grain yield decreased much more than shoot biomass (Fig. 5). These results show that drought at reproductive stages affected grain production more strongly than vegetative growth. Paul et al. (2024)[59] reported similar results in barley, showing a possible separation between biomass and grain production, where plants with relatively high biomass can still produce grain and therefore have a low HI. This pattern was particularly clear at GR in our study. ASi and control treatments did not differ significantly; however, ASi-treated pots produced significantly higher grain and HI. Therefore, the ASi benefit cannot be explained by greater plant growth, but rather by ASi helping the plant maintain grain production under drought during reproductive stages. This grain yield preservation is consistent with our physiological data (e.g., LWP, ABA, g_s). All these results combined support the idea that ASi helped plants remain active during drought, reduced the risk of early senescence, and maintained grain production, especially when drought occurred during reproductive phenological stages. Our findings also align with Ning et al. (2023)[60], who reported that ASi application reduced drought-related yield loss during anthesis and grain filling in wheat. In contrast, drought during ST did not reduce yield in either treatment. Although ASi-treated plants showed slightly higher yields than the control, the differences were not significant. Under mild drought, ASi did not provide an extra yield advantage, as plants in both treatments recovered fully after rewetting.

In addition to the dependence of drought timing on ASi's drought-mitigation potential, we could disentangle the distinct effects of ASi on soil water availability (the ASi-soil effect) and on plant physiology via ASi accumulation in leaves (the ASi-plant effect). Here, we also observed temporal plasticity in the prevailing dominance of both processes. Although the ASi benefit was consistent, the dominant mechanism likely shifted over time, reflecting two pathways: an ASi-soil effect and an ASi-plant effect.

The ASi-soil effect refers to improvements in soil physical properties, including enhanced soil water retention and hydraulic conductivity, which delay the onset of critical water limitation [19,52]. The ASi-plant effect refers to the effect of ASi on plant regulation and physiological and hormonal responses to drought, including stomatal regulation and ABA biosynthesis[61,62]. These plant-level adjustments interact with soil-level improvements. For example, when soil moisture remains available for longer, plants delay crossing the hydraulic and hormonal thresholds that trigger rapid stomatal closure and the subsequent decline in carbon assimilation.

The drought at ST offers the clearest example of an ASi-plant effect. ET was reduced in both treatments, with no significant differences, and SWC remained similar across treatments throughout the drought (Figs. 1 and 2). Thus, ASi did not increase the amount of water retained in the soil or reduce the rate of water loss during the drought at ST, ruling out the influence of the ASi-soil effect. Moreover, despite similar SWC, ASi-treated pots showed more negative SMP, which became significantly more negative during the last two days of drought (Fig. 1E). This indicates that, at similar SWC, water was held under greater tension in the ASi-treated pots. Yet on the final drought day, as drought became more critical, ASi-treated pots showed better plant water status (less negative LWP) and more open stomata (higher g_s). These late differences indicate that ASi modified plant drought responses as drought severity increased. The ABA-SMP relationship (Fig. 3) reinforces this interpretation. SMP reflects the energetic barrier that the plant faces in extracting water from the soil [53,54]. In this relationship, a less steep ABA-SMP slope under ASi means that the plant accumulated less ABA for the same increase in soil water limitation. Because SWC did not differ between treatments, the weaker ABA response cannot be explained by ASi-soil effect (increasing soil water storage) and instead points to altered

ABA balance via changes in production and breakdown. The LWP-SMP and g_s-SMP relationships support the same interpretation. At a given SMP, ASi-treated plants generally maintained a less negative LWP and higher gs than the control, especially as soil water limitation became stronger. This means that the same increase in soil water stress translated into a weaker decline in plant water status and stomatal opening under ASi. Together with the less steep ABA-SMP relationship, these patterns suggest that ASi reduced the physiological sensitivity of barley to declining soil water availability, consistent with an ASi-plant effect. This interpretation is consistent with cereal studies showing that ASi supply can reduce ABA accumulation under water deficit while supporting gas exchange and plant water status [27,63,64]. For example, in barley, ASi reduced ABA under osmotic stress and was linked to transcriptional regulation of ABA metabolism [27]. In wheat, ASi reduced ABA and improved water status under deficit conditions[64], and in sorghum ASi improved water relations and delayed stomatal closure that would otherwise prevent hydraulic failure [63].

However, a hydraulic contribution cannot be excluded completely. The same SMP does not necessarily imply the same hydraulic conductivity, and ASi could maintain higher unsaturated hydraulic conductivity as soil dries[52]. Greater soil hydraulic conductivity should improve water delivery from the soil to the root and delay the hydraulic conductivity signals associated with stomatal closure and ABA accumulation[65,66]. Our measurements cannot distinguish this mechanism from a direct physiological effect of ASi within the plant. Therefore, the plant response at ST is most consistent with a dominant ASi-plant effect, while a contribution from altered soil hydraulic conductivity remains possible.

The drought at FL and GR points mainly to the ASi-soil effect. ET declined after drought onset in both treatments, but ASi-treated pots sustained significantly higher ET than controls, matching the consistently higher SWC under ASi (Figs. 1 and 2). This coupling of high ET and SWC is important because it shows that higher ET under ASi did not reflect faster dehydration, but rather better access to soil water and weaker drought signaling, reflected in less negative LWP and lower ABA levels in plant leaves in ASi-treated plants (Figs. 2–4). NEE showed the same trend as ET. ASi-treated pots showed higher CO_2 uptake (as also shown by higher gs), and the drop occurred later than in the control, which dropped right after drought started. Overall, ASi delayed the time of crossing a stress threshold, where stomatal limitation intensifies, and plant water status declines. Our findings also align with previous studies showing that enhancing water availability via ASi can alleviate drought stress and sustain better water status under drought conditions [52,67].

While this study suggests that ASi as a soil amendment may improve plant performance under acute drought pulses, future research should explore the scalability of these effects under chronic, field-representative water deficits. Furthermore, investigating alternative delivery mechanisms -such as targeted foliar applications- could optimize ASi uptake and provide more flexible management strategies across varying agricultural environments.

Conclusion

ASi does not significantly boost yield in non-drought-stress conditions. Its primary value is in safeguarding yield during severe drought. During mild and reversible drought, plants fully recover, and ASi offers no clear benefit. However, when water shortages coincide with sensitive reproductive phases, ASi helps maintain plant function and prevent permanent yield loss. This protection mainly delays the onset of critical physiological

stress rather than removing the impacts of drought. The effectiveness of ASi depends heavily on the timing and intensity of drought. Therefore, its positive effects, drought-mitigating-wise, are most noticeable under severe drought stress and during drought-sensitive stages, making ASi management a prone tool for more sustainability in agriculture under currently predicted climate change scenarios with more pronounced and more frequent drought events [57].

Declarations

Competing interest:

None declared.

Author Contribution

WH: conceptualization, conducting the experiment, data treatment and analysis, Visualization, writing the original draft, reviewing, and editing. MH: conceptualization, data analysis, Writing-review, and editing. JS: Writing-review, and editing. RR: data analysis, Writing-review, and editing. AD: Writing-review, and editing. MD: conceptualization, Writing-review, and editing.

Acknowledgement

This research has been supported by the Leibniz Society Germany for their funding through the Leibniz Cooperative Excellence program (K378/2021), awarded to Joerg Schaller and Maren Dubbert. We used ChatGPT and Grammarly Pro (v1.2.212) to check for grammar and enhance language quality.

Data Availability

All the data outputs of this study are openly available in the following repository: https://doi.org/10.4228/zalf-r4p5-8c35

References

1. Brás, T. A., Seixas, J., Carvalhais, N. & Jägermeyr, J. Severity of drought and heatwave crop losses tripled over the last five decades in Europe. *Environ. Res. Lett.* **16**, 065012 (2021).
2. Kraklow, V. A. et al. Impact of drought on global food security by 2050. *Nature Communications* (2025). https://www.nature.com/articles/s41467-025-67862-7
3. Farooq, M., Hussain, M. & Siddique, K. H. M. Drought Stress in Wheat during Flowering and Grain-filling Periods. *CRC. Crit. Rev. Plant Sci.* **33**, 331–349 (2014).
4. Zhang, J. et al. Effect of drought on agronomic traits of rice and wheat: A meta-analysis. *Int. J. Environ. Res. Public Health*. **15**, 839 (2018).

5. Daryanto, S., Wang, L. & Jacinthe, P. A. Global synthesis of drought effects on maize and wheat production. *PloS one*. **11**, e0156362 (2016).
6. Abid, M. et al. Physiological and biochemical changes during drought and recovery periods at tillering and jointing stages in wheat (Triticum aestivum L). *Sci. Rep.* **8**, 4615 (2018).
7. Lakhneko, O. et al. Transient drought during flowering modifies the grain proteome of bread winter wheat. *Front. Plant Sci.* **14**, 1181834 (2023).
8. Schaller, J. et al. The importance of reactive silica for maintaining soil health. *Plant. Soil.* **513**, 1651–1662 (2025).
9. Debona, D., Rodrigues, F. A. & Datnoff, L. E. Silicon's Role in Abiotic and Biotic Plant Stresses. *Annu. Rev. Phytopathol.* **55**, 85–107 (2017).
10. Bakhat, H. F. et al. Silicon mitigates biotic stresses in crop plants: A review. *Crop Prot.* **104**, 21–34 (2018).
11. Coskun, D. et al. The controversies of silicon's role in plant biology. *New Phytol.* **221**, 67–85 (2019).
12. Pavlovic, J., Kostic, L., Bosnic, P., Kirkby, E. A. & Nikolic, M. Interactions of silicon with essential and beneficial elements in plants. *Front. Plant Sci.* **12**, 697592 (2021).
13. Katz, O., Puppe, D., Kaczorek, D., Prakash, N. B. & Schaller J. Silicon in the Soil–Plant Continuum: Intricate Feedback Mechanisms within Ecosystems. *Plants* **10**, 652 (2021).
14. Shaw, K. et al. The beneficial impact of silicon on wheat drought resilience is dependent on cultivar and stress intensity. *Front Plant. Sci* **16**, (2025).
15. Clymans, W., Struyf, E., Govers, G., Vandevenne, F. & Conley, D. J. Anthropogenic impact on amorphous silica pools in temperate soils. *Biogeosciences* **8**, 2281–2293 (2011).
16. Struyf, E. et al. Historical land use change has lowered terrestrial silica mobilization. *Nat. Commun.* **1**, 129 (2010).
17. Vandevenne, F. I. et al. Landscape cultivation alters δ30Si signature in terrestrial ecosystems. *Sci. Rep.* **5**, 7732 (2015).
18. Puppe, D., Kaczorek, D., Schaller, J., Barkusky, D. & Sommer, M. Crop straw recycling prevents anthropogenic desilication of agricultural soil–plant systems in the temperate zone–Results from a long-term field experiment in NE Germany. *Geoderma* **403**, 115187 (2021).
19. Schaller, J., Cramer, A., Carminati, A. & Zarebanadkouki, M. Biogenic amorphous silica as main driver for plant available water in soils. *Sci. Rep.* **10**, 2424 (2020).
20. Schaller, J., Frei, S., Rohn, L. & Gilfedder, B. S. Amorphous silica controls water storage capacity and phosphorus mobility in soils. *Front. Environ. Sci.* **8**, 94 (2020).
21. Zarebanadkouki, M., Hosseini, B., Gerke, H. H. & Schaller, J. Amorphous silica amendment to improve sandy soils' hydraulic properties for sustained plant root access under drying conditions. *Front. Environ. Sci.* **10**, 935012 (2022).
22. Tripathi, P., Subedi, S., Khan, A. L., Chung, Y. S. & Kim, Y. Silicon effects on the root system of diverse crop species using root phenotyping technology. *Plants* **10**, 885 (2021).
23. David, O. A. et al. Complexation and immobilization of arsenic in maize using green synthesized silicon nanoparticles (SiNPs). *Sci. Rep.* **14**, 6176 (2024).

24. Liu, P. et al. Enhanced root hydraulic conductance by aquaporin regulation accounts for silicon alleviated salt-induced osmotic stress in Sorghum bicolor L. *Environ. Exp. Bot.* **111**, 42–51 (2015).
25. Chen, D. et al. Silicon moderated the K deficiency by improving the plant-water status in sorghum. *Sci. Rep.* **6**, 22882 (2016).
26. Shi, Y. et al. Silicon enhances water stress tolerance by improving root hydraulic conductance in Solanum lycopersicum L. *Front. Plant Sci.* **7**, 196 (2016).
27. Maillard, A. et al. Silicon transcriptionally regulates sulfur and ABA metabolism and delays leaf senescence in barley under combined sulfur deficiency and osmotic stress. *Environ. Exp. Bot.* **155**, 394–410 (2018).
28. Mukarram, M. et al. Beyond essentiality: silicon as a systems regulator of photosynthesis under stress scenarios. *Front. Plant Sci.* **16**, 1690421 (2025).
29. Ning, D. et al. Silicon-mediated physiological and agronomic responses of maize to drought stress imposed at the vegetative and reproductive stages. *Agronomy* **10**, 1136 (2020).
30. Raza, M. A. S. et al. Morpho-physiological and biochemical response of wheat to various treatments of silicon nano-particles under drought stress conditions. *Sci. Rep.* **13**, 2700 (2023).
31. Hamwi, A. A low-cost, automatic soil–plant–atmosphere enclosure system to investigate CO 2 and evapotranspiration flux dynamics. *Biogeosciences* **21**, 5639–5651 (2024).
32. Stein, M., Puppe, D., Kaczorek, D., Buhtz, C. & Schaller, J. Silicon extraction from x-ray amorphous soil constituents: a method comparison of alkaline extracting agents. *Front. Environ. Sci.* **12**, 1389022 (2024).
33. Shrestha, A. et al. Natural diversity uncovers *P5CS1* regulation and its role in drought stress tolerance and yield sustainability in barley. *Plant. Cell. Environ.* **45**, 3523–3536 (2022).
34. Passioura, J. B. The transport of water from soil to shoot in wheat seedlings. *J. Exp. Bot.* **31**, 333–345 (1980).
35. Li, X., Wilkinson, S., Shen, J., Forde, B. G. & Davies, W. J. Stomatal and growth responses to hydraulic and chemical changes induced by progressive soil drying. *J. Exp. Bot.* **68**, 5883–5894 (2017).
36. Šimura, J. et al. Plant hormonomics: multiple phytohormone profiling by targeted metabolomics. *Plant Physiol.* **177**, 476–489 (2018).
37. Eggert, K. Von Wirén, N. Response of the plant hormone network to boron deficiency. *New Phytol.* **216**, 868–881 (2017).
38. Hoffmann, M. et al. Automated modeling of ecosystem CO2 fluxes based on periodic closed chamber measurements: A standardized conceptual and practical approach. *Agric. For. Meteorol.* **200**, 30–45 (2015).
39. Dahlmann, A. et al. Benefits of a robotic chamber system for determining evapotranspiration in an erosion-affected, heterogeneous cropland. *Hydrol. Earth Syst. Sci.* **27**, 3851–3873 (2023).
40. Webb, E. K., Pearman, G. I. & Leuning, R. Correction of flux measurements for density effects due to heat and water vapour transfer. *Quart. J. Royal Meteoro Soc.* **106**, 85–100 (1980).
41. Hupp, J. The importance of water vapor measurements and corrections. *LI-COR Biosci. Inc Application Note*. **129**, 8 (2011).

42. Lloyd, J. & Taylor, J. A. On the temperature dependence of soil respiration. *Functional ecology* 315–323 (1994).
43. Elsgaard, L. et al. Net ecosystem exchange of CO2 and carbon balance for eight temperate organic soils under agricultural management. *Agric. Ecosyst. Environ.* **162**, 52–67 (2012).
44. Wang, K. et al. Comparison between eddy covariance and automatic chamber techniques for measuring net ecosystem exchange of carbon dioxide in cotton and wheat fields. *Biogeosciences* **10**, 6865–6877 (2013).
45. Gilmanov, T. G. et al. Partitioning European grassland net ecosystem CO2 exchange into gross primary productivity and ecosystem respiration using light response function analysis. *Agric. Ecosyst. Environ.* **121**, 93–120 (2007).
46. Gilmanov, T. G. et al. CO2 uptake and ecophysiological parameters of the grain crops of midcontinent North America: Estimates from flux tower measurements. *Agric. Ecosyst. Environ.* **164**, 162–175 (2013).
47. Anapalli, S. S., Pinnamaneni, S. R., Chastain, D. R., Reddy, K. N. & Simmons, C. D. Eddy covariance quantification of carbon and water dynamics in twin-row vs. single-row planted corn. *Agric. Water Manage.* **281**, 108235 (2023).
48. Zhang, G., Leclerc, M. Y., Poudel, K., Tubbs, R. S. & Monfort, W. S. Impact of peanut seeding rate on water-use efficiency and yield. *Front. Agron.* **7**, 1514588 (2025).
49. Mutanda, M., Figlan, S., Chaplot, V., Madala, N. E. & Shimelis, H. Selection of Wheat (Triticum aestivum L.) Genotypes Using Yield Components, Water Use Efficiency and Major Metabolites Under Drought Stress. *J. Agron. Crop. Sci.* **210**, e12766 (2024).
50. Puppe, D., Kaczorek, D., Buhtz, C. & Schaller, J. The potential of sodium carbonate and Tiron extractions for the determination of silicon contents in plant samples—A method comparison using hydrofluoric acid digestion as reference. *Front. Environ. Sci.* **11**, 1145604 (2023).
51. Schaller, J. et al. Increased wheat yield and soil C stocks after silica fertilization at the field scale. *Sci. Total Environ.* **887**, 163986 (2023).
52. Zarebanadkouki, M., Hamwi, A., Abdalla, W., Rahnemaie, M., Schaller, J. & R. & The effect of amorphous silica on soil–plant–water relations in soils with contrasting textures. *Sci. Rep.* **14**, 10277 (2024).
53. Hillel, D. *Introduction to Environmental Soil Physics* (Elsevier, 2003).
54. De Swaef, T. et al. On the pivotal role of water potential to model plant physiological processes. *silico Plants*. **4**, diab038 (2022).
55. Juenger, T. E. & Verslues, P. E. Time for a drought experiment: do you know your plants' water status? *Plant. Cell.* **35**, 10–23 (2023).
56. Kunz, J., Räder, A. & Bauhus, J. Effects of drought and rewetting on growth and gas exchange of minor European broadleaved tree species. *Forests* **7**, 239 (2016).
57. Schaller, J., Webber, H., Ewert, F., Stein, M. & Puppe, D. The transformation of agriculture towards a silicon improved sustainable and resilient crop production. *npj Sustainable Agric.* **2**, 27 (2024).
58. Yang, J. C., Zhang, J. H., Wang, Z. Q., Zhu, Q. S. & Liu, L. J. Involvement of abscisic acid and cytokinins in the senescence and remobilization of carbon reserves in wheat subjected to water stress during grain filling. *Plant. Cell. Environ.* **26**, 1621–1631 (2003).

59. Paul, M., Dalal, A., Jääskeläinen, M., Moshelion, M. & Schulman, A. H. Precision phenotyping of a barley diversity set reveals distinct drought response strategies. *Front. Plant Sci.* **15**, 1393991 (2024).
60. Ning, D. et al. The effects of foliar supplementation of silicon on physiological and biochemical responses of winter wheat to drought stress during different growth stages. *Plants* **12**, 2386 (2023).
61. Vandegeer, R. K. et al. Silicon deposition on guard cells increases stomatal sensitivity as mediated by K+ efflux and consequently reduces stomatal conductance. *Physiol. Plant.* **171**, 358–370 (2021).
62. Mukarram, M. et al. Silicon nanoparticles in higher plants: Uptake, action, stress tolerance, and crosstalk with phytohormones, antioxidants, and other signalling molecules. *Environ. Pollut.* **310**, 119855 (2022).
63. Hattori, T. et al. Application of silicon enhanced drought tolerance in *Sorghum bicolor*. *Physiol. Plant.* **123**, 459–466 (2005).
64. Xu, L. et al. Silicon and water-deficit stress differentially modulate physiology and ultrastructure in wheat (Triticum aestivum L). *3 Biotech.* **7**, 273 (2017).
65. Carminati, A. & Javaux, M. Soil Rather Than Xylem Vulnerability Controls Stomatal Response to Drought. *Trends Plant Sci.* **25**, 868–880 (2020).
66. Abdalla, M. et al. Stomatal closure during water deficit is controlled by below-ground hydraulics. *Ann. Botany*. **129**, 161–170 (2022).
67. Schaller, J. et al. Silica fertilization improved wheat performance and increased phosphorus concentrations during drought at the field scale. *Sci. Rep.* **11**, 20852 (2021).

Figures

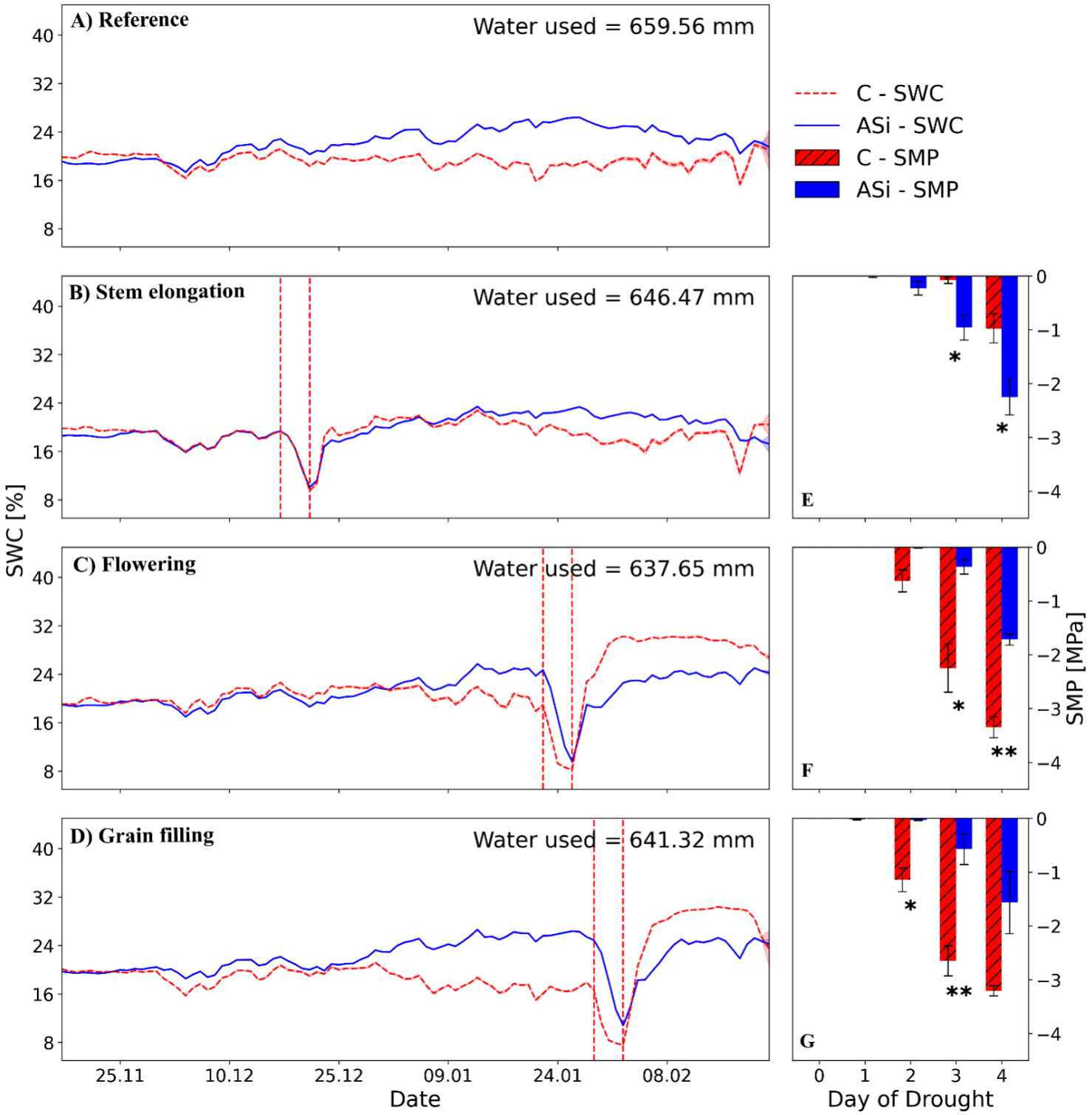


Figure 1

Averaged dynamics (n=4) of Soil water content [SWC; in %] per drought group [A) Reference, B) Stem elongation, C) Flowering, D) Grain filling] during the study period, and the corresponding Soil matric potential [SMP, in MPa] during drought periods [E: Stem elongation, F: Flowering, G: Grain filling]. The solid blue line represents the ASi treatment, and the dashed red line represents the control treatment (n=4). Total water use per pot (in mm) for each group is indicated within the panels. SMP is presented as bar plots, with striped red

bars for the control and solid blue bars for ASi. Red dashed vertical lines mark the onset and end of drought periods. Error bars indicate standard error (n = 4).

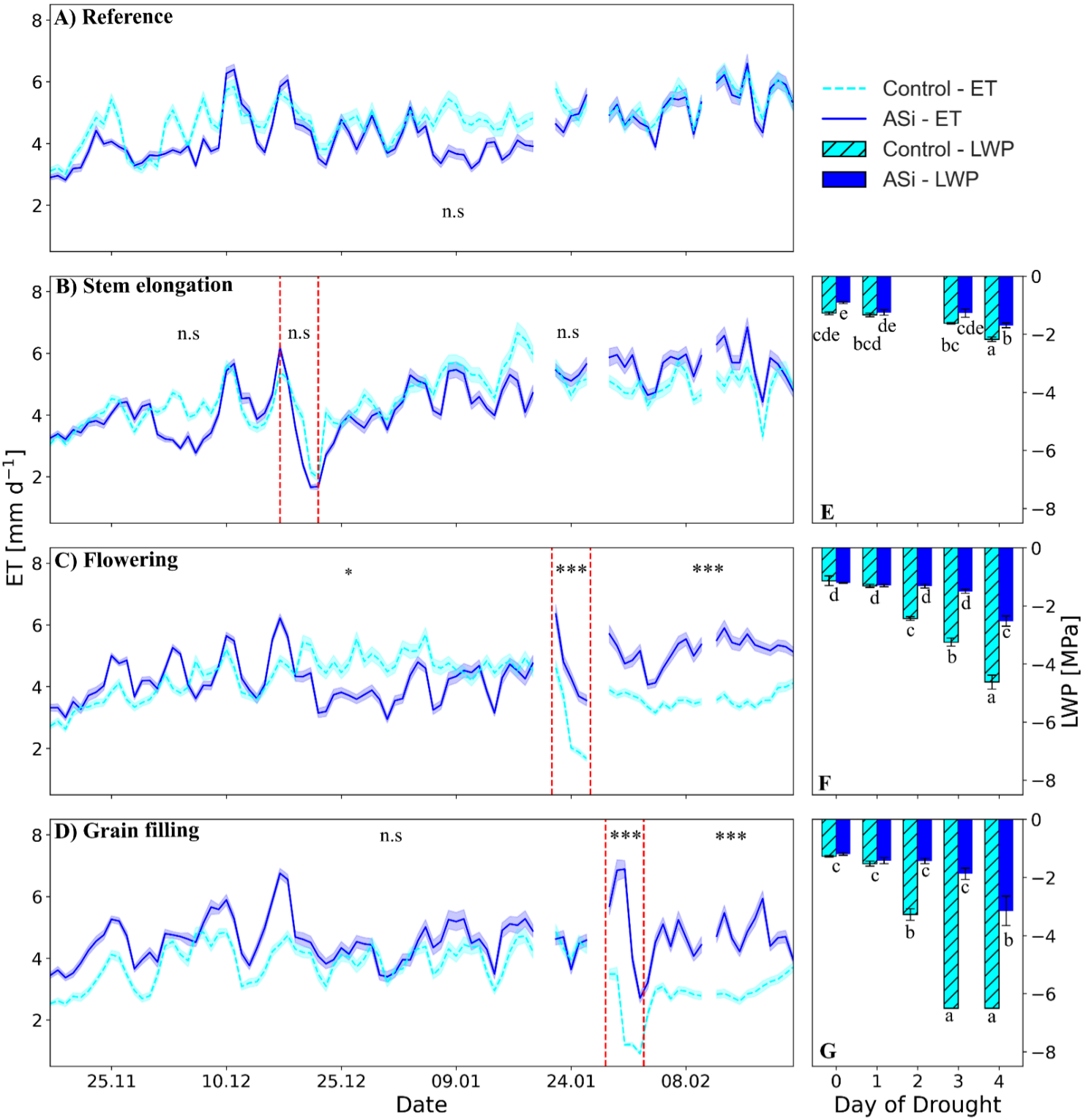


Figure 2

Dynamics of evapotranspiration (ET, mm d⁻¹) for the four different drought groups [A) Reference, B) Stem elongation, C) Flowering, D) Grain filling] during the study period, and the corresponding leaf water potential (LWP, MPa) during drought periods [E: Stem elongation, F: Flowering, G: Grain filling]. Control ET is shown as a

dashed cyan line and ASi ET as a solid blue line. Data gaps in ET reflect a lighting-system malfunction on Sundays. LWP is presented as bar plots, with striped, cyan bars for the control and solid blue bars for ASi. Red dashed vertical lines mark the onset and end of drought periods. Error bars indicate standard error (n = 4).

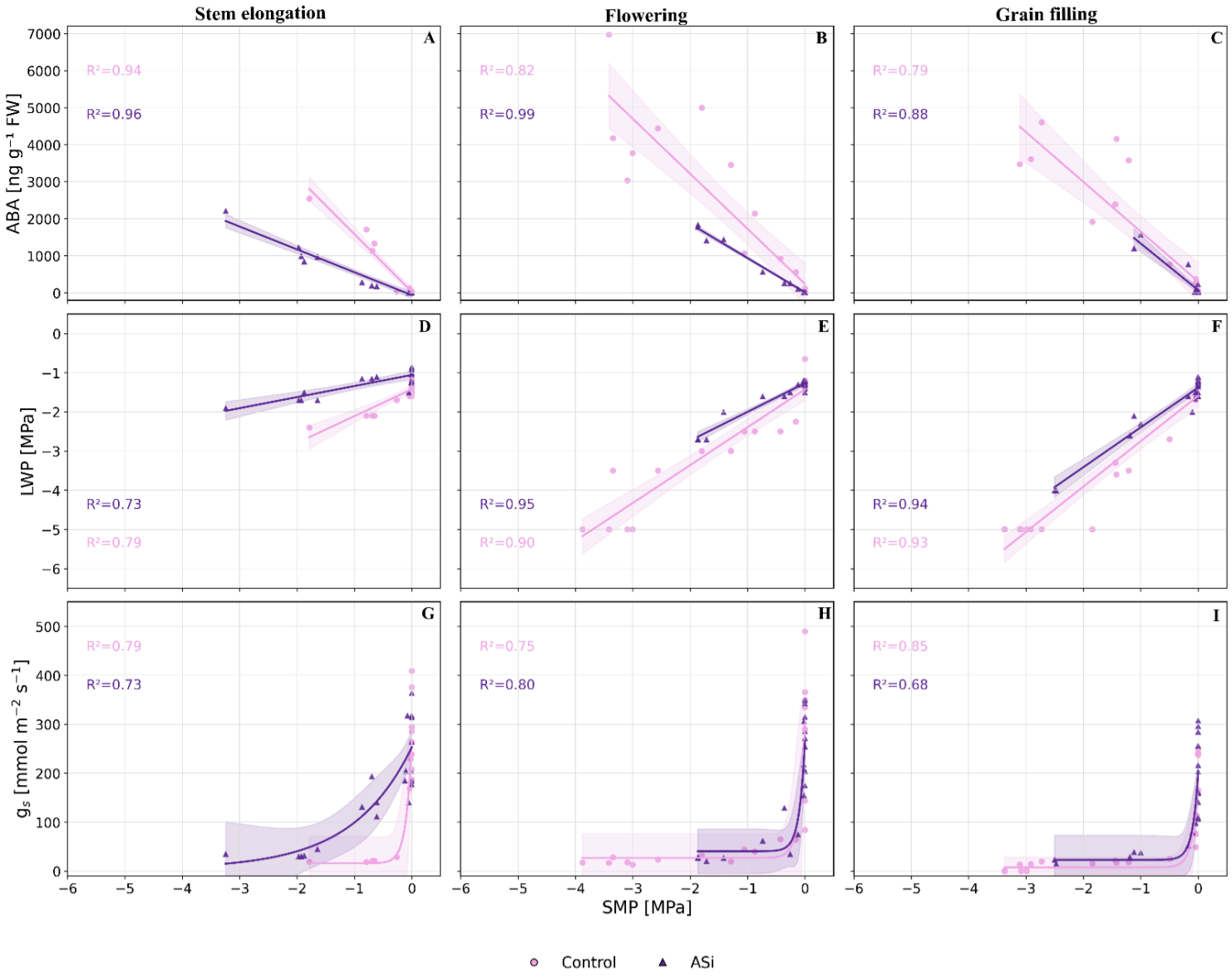


Figure 3

Response of abscisic acid concentration (ABA, ng g^{-1} FW), leaf water potential (LWP, MPa), and stomatal conductance (g_s, mmol m^{-2} s^{-1}) of Barley to declining soil matric potential (SMP, MPa) during drought at three phenological stages: stem elongation (A, D, G), flowering (B, E, H), and grain filling (C, F, I). The top row shows ABA, the middle row shows LWP, and the bottom row shows g_s. Circles indicate control plants, and triangles indicate ASi-treated plants (n = 4). Lines represent fitted relationships for each treatment within each stage, using linear regression for ABA and LWP and exponential fitting for g_s. Shaded bands show the corresponding confidence intervals, and R^2 values are reported within each panel.

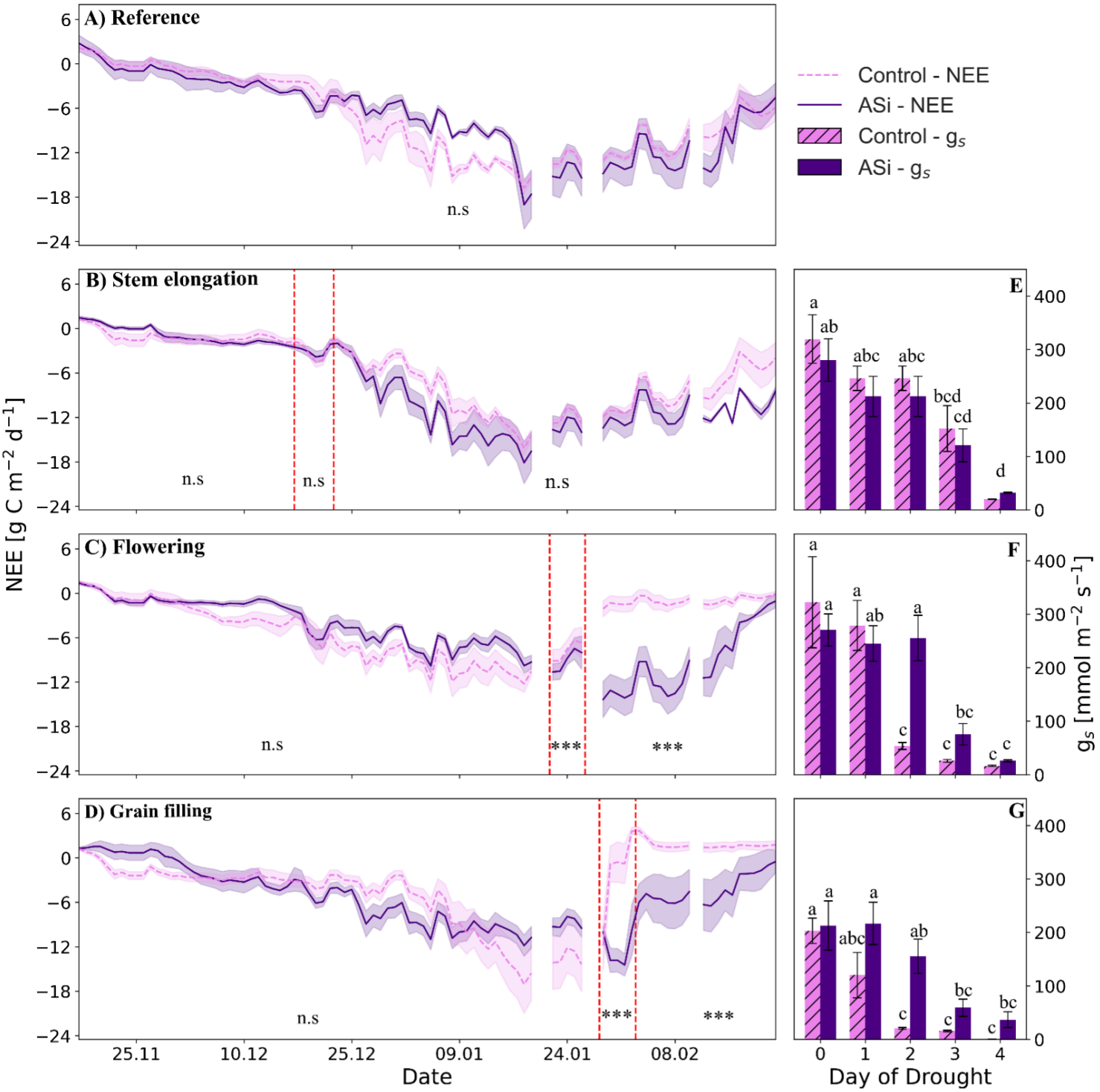


Figure 4

Dynamics of net ecosystem exchange (NEE, g C m^{-2} d^{-1}) for the four groups [A: Reference, B: Stem elongation, C: Flowering, D: Grain filling] during the study period, and the stomatal conductance (g_s, mmol m^{-2} s^{-1}) during drought periods [E: Stem elongation, F: Flowering, G: Grain filling]. Control NEE is shown as a dashed pink line and ASi NEE as a solid purple line. Data gaps in NEE reflect a lighting-system malfunction on Sundays. g_s is presented as bar plots, with striped, pink bars for the control and solid purple bars for ASi. Red dashed vertical lines mark the onset and end of drought periods. Error bars indicate standard error (n = 4).

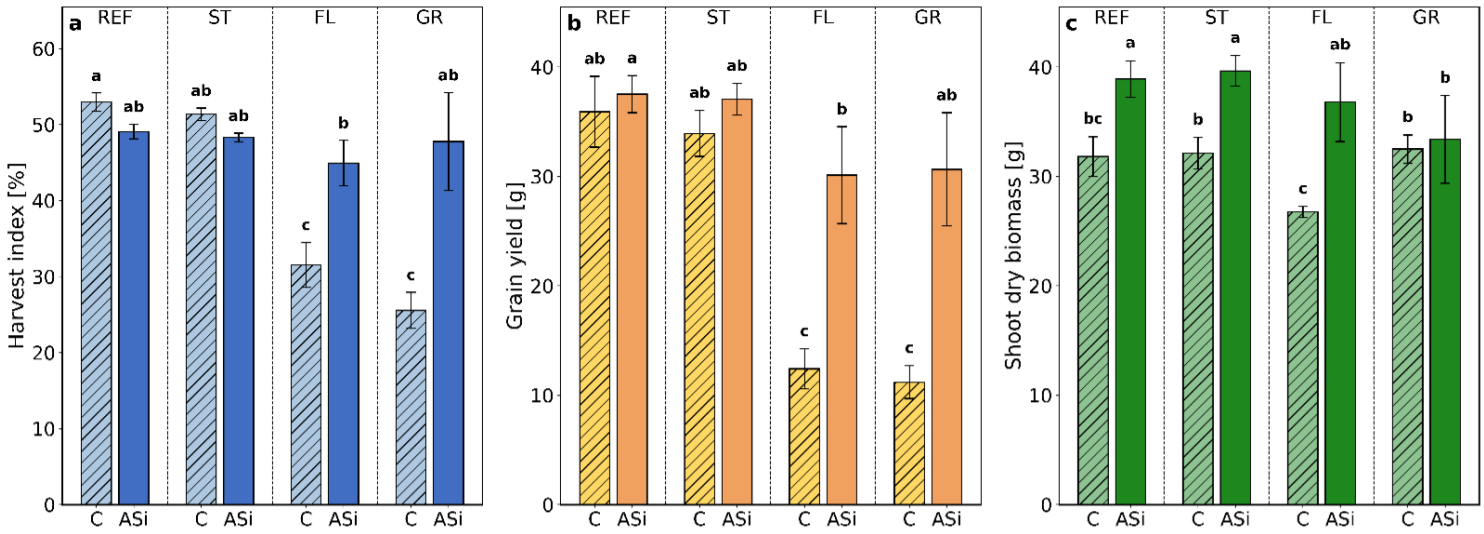


Figure 5

Harvest index (a, in %), grain yield (b, in g), and shoot dry biomass (c, in g) for the four different drought groups [REF: Reference, ST: stem elongation, FL: flowering, GR: grain filling]. Hatched bars represent the control treatment (C), and solid bars represent the ASi treatment. Error bars represent standard deviation (n = 4).

Supplementary Files

This is a list of supplementary files associated with this preprint. Click to download.

- AppendixA.docx